scientific reports

Check for updates

OPEN

Cathepsin D inhibits AGEs-induced phenotypic transformation in vascular smooth muscle cells

Xingmin He[1,9], Songhao Tian[2,9], Lixia Bu[3], Xinna Zhao[4], Liqiang Zheng[5], Peigang Zhang[6], Renwei Guo[7]✉ & Mingfeng Ma[7,8]✉

This study investigates the role of Cathepsin D (CTSD) in diabetic vascular complications, particularly its impact on the phenotypic transformation of vascular smooth muscle cells (VSMCs) induced by advanced glycation end-products (AGEs), and explores its potential molecular mechanisms. CTSD was overexpressed in VSMCs using lentiviral vectors. Various methods, including CCK-8, immunofluorescence, SA-β-Gal staining, EdU assay, scratch assay, cell cycle analysis, and Western blotting, were employed to assess VSMC viability, proliferation, migration, senescence, and apoptosis. Additionally, transcriptomic and metabolomic analyses were conducted to investigate the molecular mechanisms underlying CTSD overexpression in VSMCs. AGEs treatment significantly inhibited CTSD expression in VSMCs, leading to reduced cell viability, enhanced proliferation and migration, increased senescence, and apoptosis. In contrast, overexpression of CTSD effectively inhibited AGEs-induced VSMCs proliferation, migration, senescence, and apoptosis. Combined transcriptomic and metabolomic analyses suggested that CTSD may affect VSMCs phenotypic transformation by inhibiting the glycolysis pathway. This study highlights the critical role of CTSD in the phenotypic transformation of VSMCs induced by AGEs and provides a new perspective for cardiovascular and cerebrovascular disease treatment. CTSD may emerge as a novel therapeutic target, though its specific molecular mechanisms and clinical application prospects in VSMCs phenotypic transformation require further investigation.

Keywords Cathepsin D (CTSD), Advanced glycation end-products (AGEs), Vascular smooth muscle cells (VSMCs), Phenotypic transformation, Transcriptomics and metabolomics analysis

Diabetic vascular complications are a common and serious health issue for diabetes patients. If left unmanaged, they can lead to severe clinical outcomes such as cardiovascular events, renal failure, vision loss, and neurological impairments, significantly affecting patients' quality of life and life expectancy[1]. Insulin resistance induced by diabetes and the resulting oxidative stress are key factors driving the progression of cardiovascular and cerebrovascular diseases. These pathological changes significantly increase the risk of cardiovascular events in diabetes patients[2]. In a hyperglycemic state, the production of advanced glycation end-products (AGEs) increases. AGEs activate various signaling pathways through interaction with the receptor for advanced glycation end-products (RAGE), leading to inflammation, oxidative stress, and metabolic disturbances, which in turn promote the development of diabetic complications[3]. Dysfunction of vascular smooth muscle cells (VSMCs) is a critical risk factor for cardiac metabolic diseases. In the pathogenesis of atherosclerosis (AS), increased levels of AGEs in diabetes enhance the interaction between AGEs and their receptor RAGE, which significantly promotes the development of AS by regulating VSMCs proliferation and migration[4]. AGEs induce VSMCs apoptosis by activating NAD(P)H oxidase and increasing ROS production, a process closely related to the development of vascular calcification[5]. VSMCs play a crucial role in the progression of cardiovascular diseases.

[1]Fenyang College of Shanxi Medical University, Fenyang 032200, Shanxi, China. [2]Department of Medical Laboratory Science, Fenyang College of Shanxi Medical University, Fenyang 032200, Shanxi, China. [3]Department of Geratology, Fenyang Hospital of Shanxi Province, Fenyang 032200, Shanxi, China. [4]Research Office, Fenyang Hospital of Shanxi Province, Fenyang 032200, Shanxi, China. [5]School of Public Health, Shanghai Jiao Tong University School of Medicine, Shanghai 200000, China. [6]Department of Cardiothoracic Surgery, Lvliang People's Hospital, Li Shi 033000, Shanxi, China. [7]Department of Cardiology, Fenyang Hospital of Shanxi Province, Fenyang 032200, Shanxi, China. [8]Department of Internal Medicine, Fenyang College of Shanxi Medical University, Fenyang 032200, Shanxi, China. [9]Xingmin He and Songhao Tian have contributed equally to this work. ✉email: grw_0303@163.com; mamingfeng106@sina.com

They can transition from a contractile phenotype that maintains vascular structure to a synthetic phenotype that participates in disease processes in response to vascular wall damage or stress. This transition involves enhanced cell proliferation, migration, and the synthesis of extracellular matrix (ECM), contributing to pathological processes such as atherosclerosis, intimal hyperplasia, aneurysm formation, and vascular calcification[6].

Cathepsin D (CTSD) is a crucial aspartic protease primarily responsible for protein degradation in the acidic environment of lysosomes. It plays a significant role in regulating apoptosis, promoting wound healing, angiogenesis, and tumor invasion[7]. Studies have shown that AGEs promote the phenotypic transformation and proliferation of VSMCs in a concentration-dependent manner, partly by inhibiting CTSD. This effect can be mitigated by the specific RAGE inhibitor FPS-ZM1. Overexpression of CTSD can significantly counteract the effects of AGEs, whereas CTSD knockdown exacerbates AGE-induced p-ERK activation, highlighting CTSD's role in regulating phosphorylated ERK levels and VSMCs proliferation induced by the AGE/RAGE axis[8]. Our previous research found that AGEs inhibit VSMCs autophagy by reducing CTSD expression, thereby promoting VSMCs proliferation[9]. Conversely, overexpression of CTSD effectively prevents this process. Therefore, we hypothesize that overexpressing CTSD may influence VSMCs proliferation and migration, potentially providing a new target for the treatment of diabetic vascular complications.

Glycolysis plays a critical role in the phenotypic transformation of VSMCs. PKM2, a key rate-limiting enzyme in glycolysis, promotes VSMCs proliferation and migration when its expression and activity are upregulated. This process can be stimulated by ox-LDL and inhibited by the specific PKM2 inhibitor, Shikonin, identifying PKM2-dependent glycolysis as a potential therapeutic target for atherosclerosis progression[10]. Kruppel-like factor 4 (KLF4) enhances glycolysis by upregulating the expression of 6-phosphofructo-2-kinase (PFKFB3)[11]. It also promotes the phenotypic transformation of VSMCs through the synergistic effects of eEF1A2 and circCTDP1. This glycolysis-mediated transformation is crucial for the development of atherosclerosis. Inhibiting glycolysis can block KLF4-induced VSMCs transformation, confirming the significant role of glycolysis in VSMCs phenotypic changes. Integrated analysis of transcriptomics and metabolomics, which combines gene expression and cellular metabolite data, offers a comprehensive approach to understanding biological processes and systemic mechanisms. This method significantly improves predictive models in disease mechanisms and drug action studies, revealing new biological associations and serving as a crucial tool in advancing biomedical research[12].

This study found that overexpressing CTSD in VSMCs effectively inhibits the proliferation and apoptosis of VSMCs treated with AGEs, thereby delaying VSMCs aging. Integrated transcriptomic and metabolomic analysis suggests that this overexpression may regulate VSMCs phenotypic transformation by inhibiting glycolysis. These findings provide a scientific basis for more effective treatments of diabetic vascular complications and contribute to a comprehensive understanding of diabetes and its vascular complications.

Materials and methods

Materials and reagents

High-glucose DMEM medium (PYG0073), 0.25% trypsin solution (AR1007), and the CCK-8 assay kit (AR1199) were purchased from Wuhan Boster Biological Technology Co., Ltd. The penicillin-streptomycin mixture (100 x) (P1400) and the SA-β-Gal staining kit (G1580) were obtained from Solarbio Science & Technology Co., Ltd., Beijing, China. Fetal bovine serum (FBS) (SA201.01) was acquired from CellMax Technologies (Beijing) Co., Ltd., Beijing, China. Advanced glycation end products (AGEs) protein (bs-1158P) and control BSA (bs1158PC) (Derived from bovine serum, BSA is produced by reacting with ethanol aldehyde under sterile conditions, followed by extensive dialysis and purification steps.) were purchased from Beijing Bioss Biological Technology Co., Ltd., Beijing, China. Immunofluorescence (E-IR-R321) and EdU (E-CK-A377) bio-chemical kits were sourced from Elabscience Biotechnology Co., Ltd., Wuhan, China. The cell cycle biochemical assay kit (KGA9101-50) was provided by Nanjing Jiancheng Bioen-gineering Institute, Nanjing, China. The details of the antibodies used in the experiment are listed in Table 1.

Cell culture

Immortalized rat thoracic aorta A7r5 VSMC (CL-0316) was supplied by Wuhan Pulitzer Co. Ltd. in China and cultured in a 5% CO_2 incubator at 37 °C. The growth medium (GM) was DMEM medium supplemented with 10% (*v*/*v*) fetal bovine serum and 1% (*v*/*v*) penicillin/streptomycin, replaced every two days or as needed. Treatment of VSMCs with AGEs-BSA, referring to the method of de Oliveira Silva C et al., can mimic the pathological environment of high AGEs levels in diabetic patients[13]. The test group containing AGEs dissolved AGEs and BSA in sterile PBS and diluted to the appropriate concentration before use, and the remaining control group was supplemented with the same concentration of BSA as that of the AGEs group, so that the concentration of BSA was guaranteed to be consistent in all the different test groups. To investigate the effects of AGEs on rat VSMCs, the cells were incubated with various concentrations of AGEs (0, 25, 50, 100, 200, 400 μg/mL) for 24 h. To examine the impact of CTSD over-expression on AGEs-induced VSMCs, five cell groups were established: normal VSMCs treated with BSA (C-B group), empty vector-transfected VSMCs treated with BSA (N-B group), normal VSMCs treated with AGEs (C-A group), empty vector-transfected VSMCs treated with AGEs (N-A group), and overexpression-transfected VSMCs treated with AGEs (T-A group).

Overexpression of lentiviral vectors in VSMCs

The target gene CTSD-rat was first cloned into a lentiviral vector expressing GFP and packaged into an overexpression lentivirus. This lentivirus was then used to infect target cells. Stable infected cells were selected and identified under puromycin pressure (Fig. S1A). Specifically, cells were seeded into 6-well plates, the culture medium was removed, and each well was treated with diluted virus stock and 5 μg/mL Polybrene. An NC control group was also established. The plates were incubated at 37°C with 5% CO_2 for 24 h. After 24 h, the diluted virus

Antibodies	Cat no.	Company	Source	Dilution ratio
CTSD	21327-1-AP	Proteintech, Wuhan, China	Rabbit	1:10000
α-SMA	14395-1-AP	Proteintech, Wuhan, China	Rabbit	1:5000
OPN	22952-1-AP	Proteintech, Wuhan, China	Rabbit	1:1000
PCNA	10205-2-AP	Proteintech, Wuhan, China	Rabbit	1:10000
Bcl-2	26593-1-AP	Proteintech, Wuhan, China	Rabbit	1:1000
Bax	60267-1-Ig	Proteintech, Wuhan, China	Mouse	1:10000
P53	2524	Cell SignalingTechnology, USA	Mouse	1:1000
P21	Ab109199	abcam, UK	Rabbit	1:1000
β-actin	BM0627	Boster, Wuhan, China	Rabbit	1:1000
GAPDH	MF20	ABclonal Technology, Wuhan, China	Rabbit	1:10000
PKM2	A18799	ABclonal Technology, Wuhan, China	Rabbit	1:1000
PFKL	A7780	ABclonal Technology, Wuhan, China	Rabbit	1:1000
GLUT1	A11208	ABclonal Technology, Wuhan, China	Rabbit	1:1000
GCK	A6293	ABclonal Technology, Wuhan, China	Rabbit	1:1000
HRP Anti-Rabbit IgG	BA1054	Boster, Wuhan, China	Goat	1:10000
HRP Anti-Mouse IgG	BA1050	Boster, Wuhan, China	Goat	1:10000
Anti-Rabbit IgG-Cyanine3	E-AB-1010	Elabscience, Wuhan, China	Goat	1:50

Table 1. Antibodies information.

solution was removed and replaced with 2 mL of complete medium per well. The cells were further cultured at 37°C with 5% CO_2. Approximately 72 h post-infection, when the cells reached over 90% confluence, they were trypsinized and transferred to 60 mm culture dishes. When the cells in the 60 mm dishes reached over 50% confluence, they were maintained with 2.0 μg/mL puromycin. Subsequently, qRT-PCR was used to measure the mRNA expression levels of the target gene CTSD-rat in the stably infected cells, using ACTB as an internal reference. The primers were: rat-ACTB: F: 5'-CGTAAAGACCTCTATGCCAACA-3'; R: 5'-GGAGGAGCAAT GATCTTGATCT-3'. rat-CTSD: F: 5'-CGGACTATGACGGAAGTGGG-3'; R: 5'-CACCATAGTACTGGGCAT CCA-3'. qRT-PCR results showed that the expression of the target gene CTSD-rat in the over-expression stable clones was approximately 3.2 times higher compared to the NC group (Fig. S1B, C). To ensure the correct amplification of the target gene during PCR, the PCR products of the stable clones were sequenced. The sequencing results confirmed that the PCR products from the overexpression group matched the sequence of the target gene (NM_134334.3). The lentivirus stock and primer synthesis used in this experiment were provided by GenePharma Co., Ltd., Shanghai, China.

CCK-8 cell viability assay

Rat VSMCs were spread in 96-well plates at a density of 8000 cells/well with reference to Chen et al.[14]. After treatment according to the experimental requirements, CCK-8 solution was added, and the plates were incubated at 37 °C with 5% CO_2 for 20 min. The optical density (OD) was measured at 450 nm. Cell viability was calculated using the formula: Cell viability = [(OD of experimental well - OD of blank well) / (OD of control well - OD of blank well)] × 100%.

Cellular Immunofluorescence

After cell seeding, cells were fixed with 4% paraformaldehyde at room temperature for 30 min. They were then washed three times with PBS, 5 min each time. Cells were permeabilized with 0.5% Triton X-100 for 15 min, followed by three washes with PBS, 5 min each. After blocking with goat serum for 30 min, the cells were incubated with the primary antibody (1:200) overnight at 4 °C. After washing three times with PBS, 5 min each time, the cells were incubated with a fluorescent secondary antibody in the dark for 60 min. Following three washes with PBS, 5 min each, the nuclei were stained with DAPI for 5 min, washed three more times with PBS, 5 min each, and then mounted with an antifade reagent. The cells were observed and photographed under a fluorescence microscope.

SA-β-Gal staining

Add SA-β-Gal staining fixative to the cell culture medium and fix the cells at room temperature for 15 min. Wash the cells three times with PBS, 5 min each time. Then, add 1 mL of SA-β-Gal staining working solution to each well and incubate overnight at 37 °C without CO_2 until some cells turn blue. Observe and photograph the cells under a microscope and count the positive cells.

EdU assay

We used the EdU method to analyze DNA synthesis in VSMCs. According to the manufacturer's instructions, cells were incubated with EdU labeling solution at 37 °C for 2 h using the Elabscience E-Click EdU Cell Proliferation Imaging Assay Kit. The cells were then fixed with 4% paraformaldehyde at room temperature for 15 min. After washing with PBS containing 0.3% BSA (3 times, 5 min each), the cells were incubated with 0.3% Triton X-100 at room temperature for 20 min. The cells were then incubated with Click reaction solution at room

temperature in the dark for 30 min. After washing with PBS containing 0.3% BSA (3 times, 5 min each), the cells were stained with DAPI for 5 min. Following another wash, the cells were observed under a fluorescence microscope. Finally, EdU-labeled cells were counted using Image J software.

Cell scratching assay

Cells cultured in 6-well plates were used to draw a vertical line in the center of the bottom of the plate using a 200 μL pipette tip. The cells were then placed in serum-free medium and stimulated according to different experimental groups for 24 h. Cell migration was observed and photographed under a microscope at 0 and 24 h. The migration area was quantified using ImageJ software.

Cell cycle assay

Cells from each group, after digestion in 6-well plates, were transferred to 1.5 mL centrifuge tubes and collected by centrifugation at 1500 rpm for 5 min. The cell pellet was slowly resuspended in pre-chilled 75% (v/v) ethanol at -20 °C and incubated at 4 °C overnight. After fixation, the cells were resuspended in PBS and stained with a work-ing solution of RNase A and PI (1:9) at room temperature in the dark for 30 min. Finally, cell cycle distribution was analyzed using a flow cytometer with an excitation wave-length of 488 nm and an emission wavelength of 585 ± 21 nm. ModFit software was used to analyze the cell cycle distribution.

Western blotting

The cell samples were mixed with protein lysis buffer (RIPA) and incubated on ice for 20 min. The samples were then centrifuged at 12,000 rpm at 4 °C for 15 min to collect the supernatant, which contained the total cellular protein. Protein concentration was determined using the BCA assay. Proteins were then denatured at 100 °C for 5 min in a metal bath, separated by SDS-PAGE, and transferred to a PVDF membrane. The membrane was then blocked with 5% skim milk at room temperature for 2 h. The primary antibody was added and incubated overnight at 4 °C. The membrane was washed three times with TBST, 10 min each time. The secondary antibody was added and incubated on a shaker for 2 h. After washing three times with TBST, 10 min each time, the membrane was incubated with enhanced chemiluminescence (ECL) reagent and exposed using a Bio-Rad ChemDoc imaging system. Quantification was performed using ImageJ software.

RNA extraction and transcriptomics analysis

The cultured cells were examined under a microscope to ensure cell integrity and prevent RNA degradation by RNases released from damaged cells. Cells were then washed twice with pre-chilled 1×PBS to remove impurities. Appropriate amounts of Ambion TRIzol were added to isolate total RNA from each cell sample. Reverse transcription and library construction were performed by AllwegeneTech in Beijing. For each sample, 1.5 μg of RNA was used as input material, and the NEBNext® Ultra™ RNA Library Prep Kit for Illumina® was employed for library preparation, with index codes added to differentiate samples. mRNA was purified using poly-T oligonucleotide-conjugated magnetic beads, and fragmentation was carried out at high temperatures using the NEBNext First Strand Synthesis Reaction Buffer. First-strand cDNA was synthesized using random hexamer primers and M-MuLV reverse transcriptase, followed by second-strand cDNA synthesis using DNA polymerase I and RNase H. Overhang ends were converted to blunt ends using exonuclease/polymerase activity, followed by adenylation of the 3' ends. NEBNext adapters with hairpin loop structures were then ligated for subsequent hybridization. Selected cDNA fragments of 200–250 bp were purified using the AMPure XP system, followed by treatment with USER enzyme and PCR amplification. The final PCR products were purified again and quality assessed using the Agilent Bioanalyzer 2100 system. Sequencing was performed on the Illumina NovaSeq 6000 platform at Allwegene Technology in Beijing, generating 150 bp paired-end reads. Sequencing data were aligned with the reference genome, and FPKM values were calculated to quantify gene/transcript expression. Differentially expressed genes/transcripts were identified based on a p-value ≤ 0.05 and a fold change ≥ 2. These results were visualized using a volcano plot. Additionally, GO enrichment and pathway analysis were performed using the DAVID 6.7 and KEGG databases to provide a foundation for further functional annotation and exploration of biological significance.

Non-targeted metabolomic analysis

First, metabolites were extracted from cell pellets using an extraction solution composed of methanol, acetonitrile, and water in a 2:2:1 ratio, containing an isotopi-cally labeled internal standard mixture, for cell pellets with a count of 107 cells. Cells were then subjected to vortex mixing, liquid nitrogen freezing and thawing, ultrasonic treatment, and low-temperature incubation to ensure cell disruption and complete metabolite release. After high-speed centrifugation, the supernatant was used for ultra-high-performance liquid chromatography (UHPLC) separation, employing a Waters ACQUITY UPLC BEH Amide column and specific mobile phase conditions for chromatographic analysis. Next, mass spectrometry data were collected using the Orbitrap Exploris 120 mass spectrometer controlled by Xcalibur software. Parameters set included sheath gas flow, auxiliary gas flow, capillary temperature, full scan resolution, MS/MS resolution, collision energy, and spray voltage. The raw data were converted to mzXML format using ProteoWizard software. Orthogonal Partial Least Squares Dis-crimination Analysis (OPLS-DA) was employed to identify differential metabolites associated with the groups from the dataset. The criteria for selection included a p-value < 0.05 from Student's t-test, a fold change > 1.5 or < 0.67, and a Variable Importance in Projection (VIP) > 1 for the first principal component in the OPLS-DA model, used to identify differential metabolites between groups. Finally, metabolites were identified and visualized using a custom R package and the AllwegeneDB data-base.

Statistical analysis

Data are expressed as mean ± SEM. Differences between two groups or among multiple groups were analyzed using Student's t-test or one-way ANOVA with a post-hoc Tukey HSD test, performed with SPSS 20.0 (SPSS Inc., Chicago, IL, USA). A p-value < 0.05 was considered significant, and a p-value < 0.01 was considered highly significant.

Results

AGEs treatment inhibits VSMCs viability and CTSD expression

Smooth muscle actin (α-SMA) is a crucial marker for the contractile phenotype of VSMCs. Immunofluorescence confirmed that the experimental cells were indeed VSMCs (Fig. 1A). When VSMCs were treated with various concentrations of AGEs, those exposed to 200 μg/mL AGEs exhibited a change from their typical spindle or band shapes to a rounder form, with increased intercellular spaces (Fig. 1B). The CCK-8 assay revealed that treatment with 200 μg/mL AGEs significantly reduced the viability of VSMCs compared to the control group ($p < 0.01$). 400 μg/mL AGEs treatment of VSMCs observed nuclear consolidation or fragmentation in some cells, which may be a manifestation of apoptosis or necrosis induced by AGEs (Fig. 1C). Additionally, it was found that 200 μg/mL AGEs treatment significantly suppressed the expression of CTSD in VSMCs ($p < 0.01$) (Fig. 1D).

Overexpression of CTSD attenuates AGEs-induced VSMCs proliferation and migration

Based on previous experimental results, VSMCs were treated with 200 μg/mL AGEs, and a CTSD overexpression VSMC model was successfully established (Fig. 2A, B) to further investigate the role of CTSD in VSMC proliferation and migration. The CTSD overexpression group (T-A) was able to reverse the reduction in CTSD ex-pression levels observed in the AGEs-treated groups (C-A and N-A), bringing them closer to the levels seen in the control groups (C-B and N-B) (Fig. 2A, B). Compared to the control group, CTSD overexpression significantly reduced the expression of Proliferating Cell Nuclear Antigen (PCNA) ($p < 0.05$) (Fig. 2C) and the number of EdU-positive cells ($p < 0.01$) (Fig. 2D). Flow cytometry analysis of the cell cycle revealed that CTSD overexpression significantly decreased the proportion of cells in the S and G2/M phases ($p < 0.01$) and significantly increased the proportion of cells in the G0/G1 phase ($p < 0.01$) (Fig. 2E). These results suggest that CTSD overexpression effectively inhibits AGEs-induced VSMC proliferation by arresting cells in the G0/G1 phase and suppressing mitosis. Scratch assay results showed that AGEs treatment significantly increased VSMC migration rates compared to the control group ($p < 0.01$). However, compared to the AGEs-treated N-A group, CTSD overexpression reduced VSMC migration rates ($p > 0.05$) (Fig. 2F). These findings indicate that CTSD overexpression can inhibit VSMC proliferation and migration.

Overexpression of CTSD attenuates AGEs-induced senescence in VSMCs

To clarify the mechanism by which CTSD overexpression inhibits the proliferation and migration of VSMCs, we used senescence-associated β-galactosidase (SA-β-Gal) staining to study the effect of CTSD overexpression on the senescence of AGEs-treated VSMCs. The results showed that CTSD overexpression significantly reduced the number of senescent VSMCs induced by AGEs treatment (Fig. 3A). Additionally, CTSD overexpression was found to reverse the increase in senescence-associated proteins P53 and P21 in AGEs-treated VSMCs ($p < 0.01$) (Fig. 3B). These results indicate that CTSD overexpression can inhibit the senescence of VSMCs.

Overexpression of CTSD attenuates AGEs-induced apoptosis in VSMCs

The proliferation and apoptosis of VSMCs are closely related to the development of Diabetic vascular complications. Therefore, we examined the expression of apoptosis-related proteins BCL-2 and Bax. Compared to the N-A group, the Bax/BCL-2 ratio in the T-A group was significantly reduced ($p < 0.01$) (Fig. 4). These results indicate that CTSD overexpression can inhibit VSMC apoptosis.

Overexpression of CTSD affects VSMCs phenotypic transformation through α-SMA and OPN

α-Smooth muscle actin (α-SMA) and osteopontin (OPN) are closely related to the phenotypic transformation of VSMCs. Therefore, we examined the expression of α-SMA and OPN in VSMCs. AGEs treatment significantly inhibited the expression of α-SMA ($p < 0.01$) and significantly promoted the expression of OPN ($p < 0.01$) (Fig. 5). Compared to the N-A group, the T-A group showed a significant increase in α-SMA expression ($p < 0.05$) and a significant decrease in OPN expression ($p < 0.01$) (Fig. 5). These results indicate that CTSD overexpression influences the phenotypic transformation of VSMCs through α-SMA and OPN.

Effect of overexpression of CTSD on the transcriptome of VSMCs induced by ages

To better understand the mechanism by which CTSD regulates VSMC phenotypic trans-formation, we examined the effect of CTSD on the transcriptome of AGEs-induced VSMCs. In preliminary experiments, there were no significant differences between the C-B and N-B groups or the C-A and N-A groups. Therefore, we selected the N-B, N-A, and T-A groups for transcriptomic and subsequent metabolomic studies. Each sample yielded 54.35 to 64.31 million clean reads after quality control (Table S1). PCA analysis revealed significant differences in the transcriptome profiles among the N-B, N-A, and T-A groups (Fig. 6A). Differential expression analysis identified 1,046 differentially expressed genes (DEGs) between the N-B and N-A groups, including 606 upregulated genes and 440 downregulated genes (Fig. 6B). Compared to the N-A group, 2,064 DEGs were identified in the T-A group, including 930 upregulated genes and 1,134 downregulated genes (Fig. 6B). Venn diagram analysis revealed 544 DEGs common to all three groups, which may be target genes through which CTSD influences VSMC phenotypic transformation (Fig. 6C). GO and KEGG enrichment analyses were performed on these 544 DEGs to characterize the mechanisms by which CTSD affects VSMC phenotypic transformation. GO enrichment analysis showed that the biological processes were mainly enriched in metabolic processes; cellular

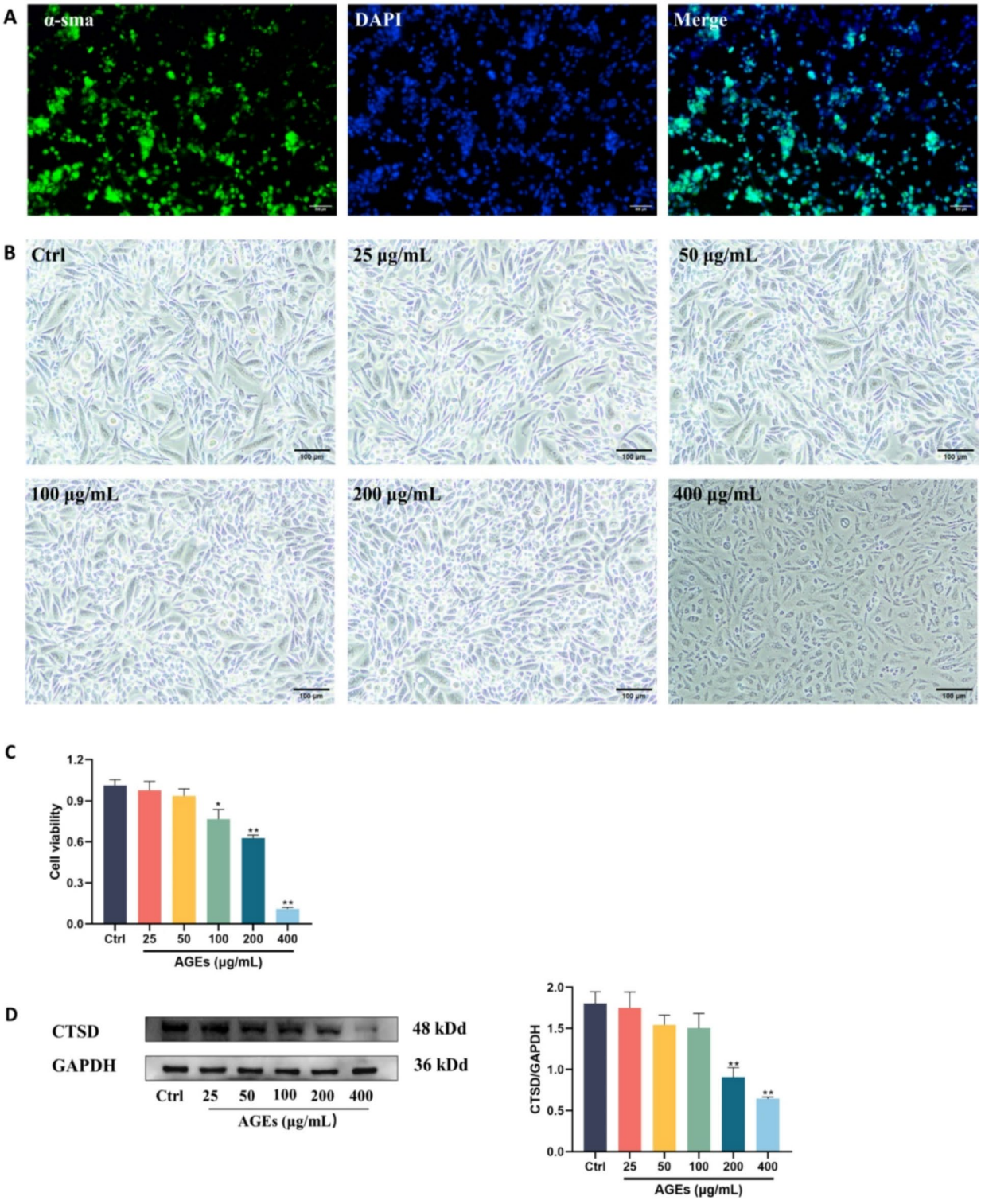

Fig. 1. AGEs treatment inhibits VSMC viability and CTSD expression. (**A**) Detection of α-SMA expression in VSMC using immunofluorescence staining (scale bar = 500 μm). (**B**) Morphological changes in VSMCs treated with different concentrations of AGEs (scale bar = 100 μm). (**C**) Effect of different concentrations of AGE on vascular endothelial cell viability as detected by cck-8. (**D**) The effects of different concentrations of AGE on CTSD expression in VSMC were examined using western blotting. All data are presented as mean ± SEM ($n = 3$). * represents $p < 0.05$, ** represents $p < 0.01$. Note: α-SMA in the figure represents Smooth muscle actin.

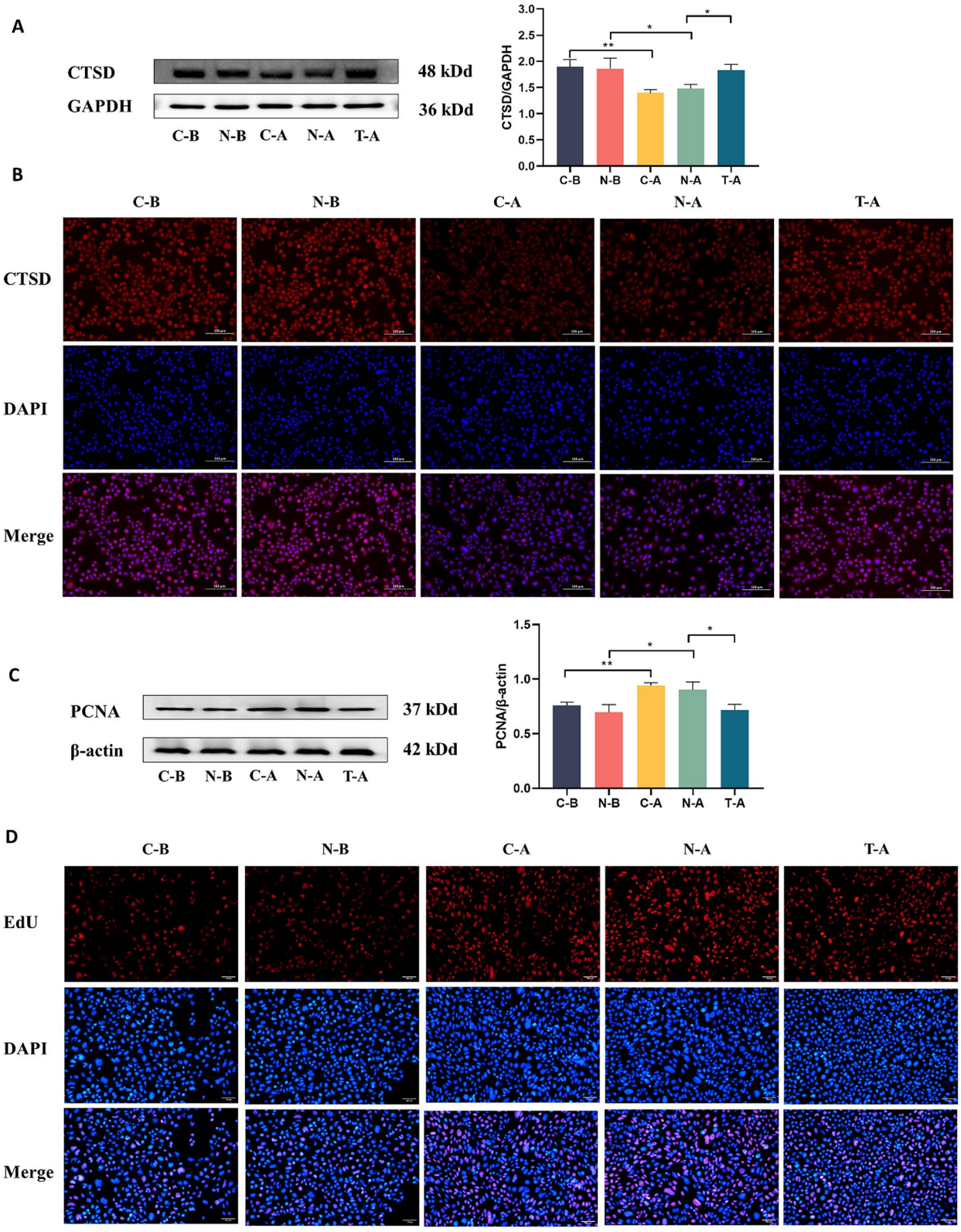

Fig. 2. Overexpression of CTSD inhibits AGEs-induced proliferation and migration of VSMCs. (**A**) Western blot analysis of the relative expression levels of CTSD in VSMCs. (**B**) Immunofluorescence staining of CTSD in VSMCs (scale bar = 100 μm). (**C**) Western blot analysis of the relative expression levels of PCNA in VSMCs. (**D**) Quantification of the percentage of EdU-positive cells; blue indicates nuclear staining and red indicates EdU staining. (**E**) Flow cytometry analysis of cell cycle distribution, with histograms showing the percentage of cells in each phase of the cell cycle. (**F**) Scratch assay results of VSMCs, with histograms showing the migration rates of cells in different groups. All data are presented as mean ± SEM ($n = 3$). * represents $p < 0.05$, ** represents $p < 0.01$. Note: PCNA in the figure represents Proliferating Cell Nuclear Antigen.

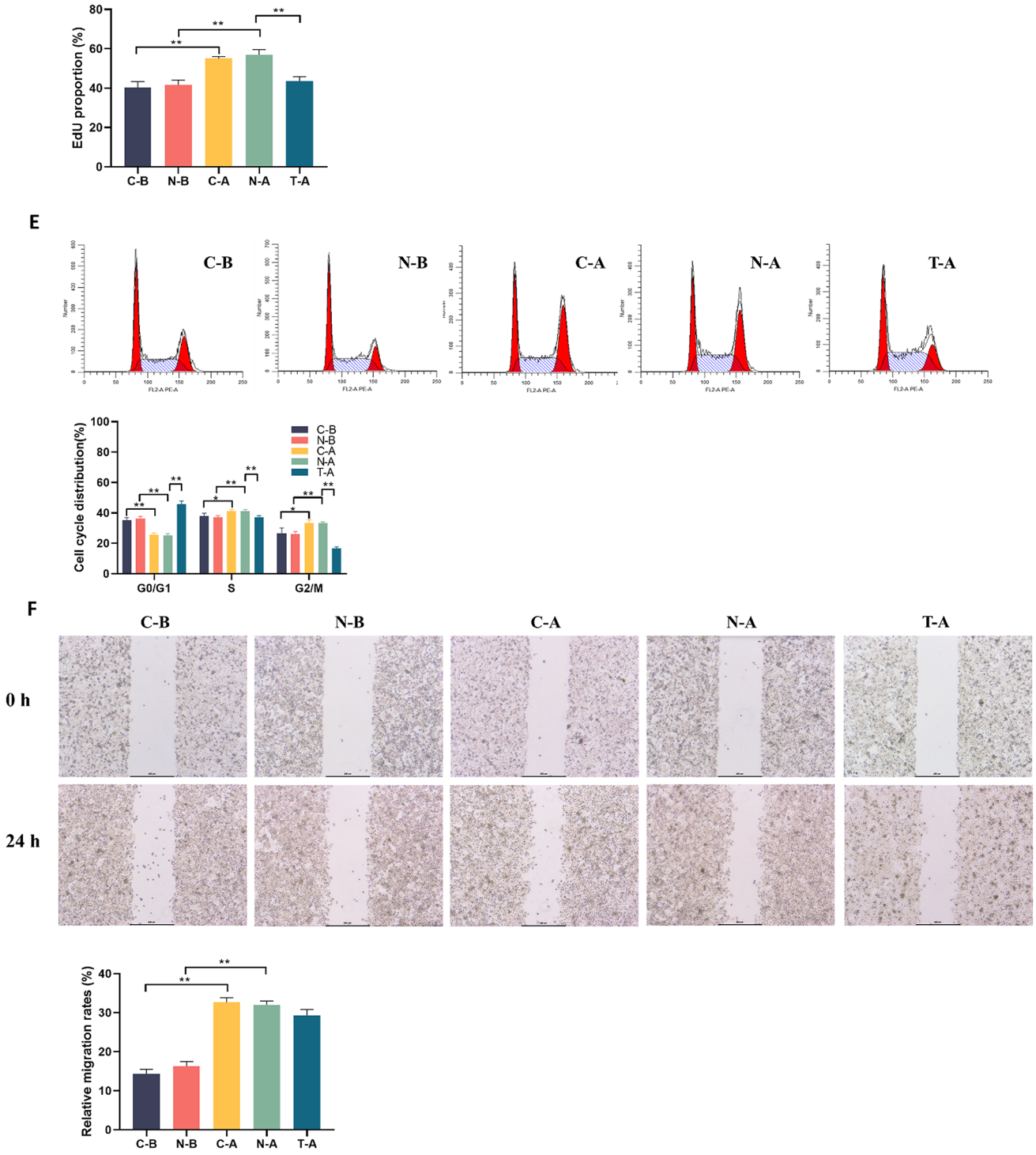

Figure 2. (continued)

components were mainly enriched in intracellular components; and molecular functions were mainly enriched in protein binding (Fig. 6D). KEGG enrichment analysis indicated that the proteasome, spliceosome, protein processing in the endoplasmic reticulum, and RNA transport pathways may be involved in the regulation of VSMC phenotypic transformation by CTSD (Fig. 6E).

Effect of overexpression of CTSD on the metabolome of VSMCs induced by ages

Additionally, we examined the effect of CTSD on the metabolomic profile of AGEs-induced VSMCs. Using UPLC-MS/MS, a total of 1,179 annotated metabolites were detected. PCA analysis revealed significant differences in the metabolomic profiles among the N-B, N-A, and T-A groups (Fig. 7A). Differential metabolite analysis identified 564 differential metabolites (DMs) between the N-B and N-A groups, including 318 upregulated and

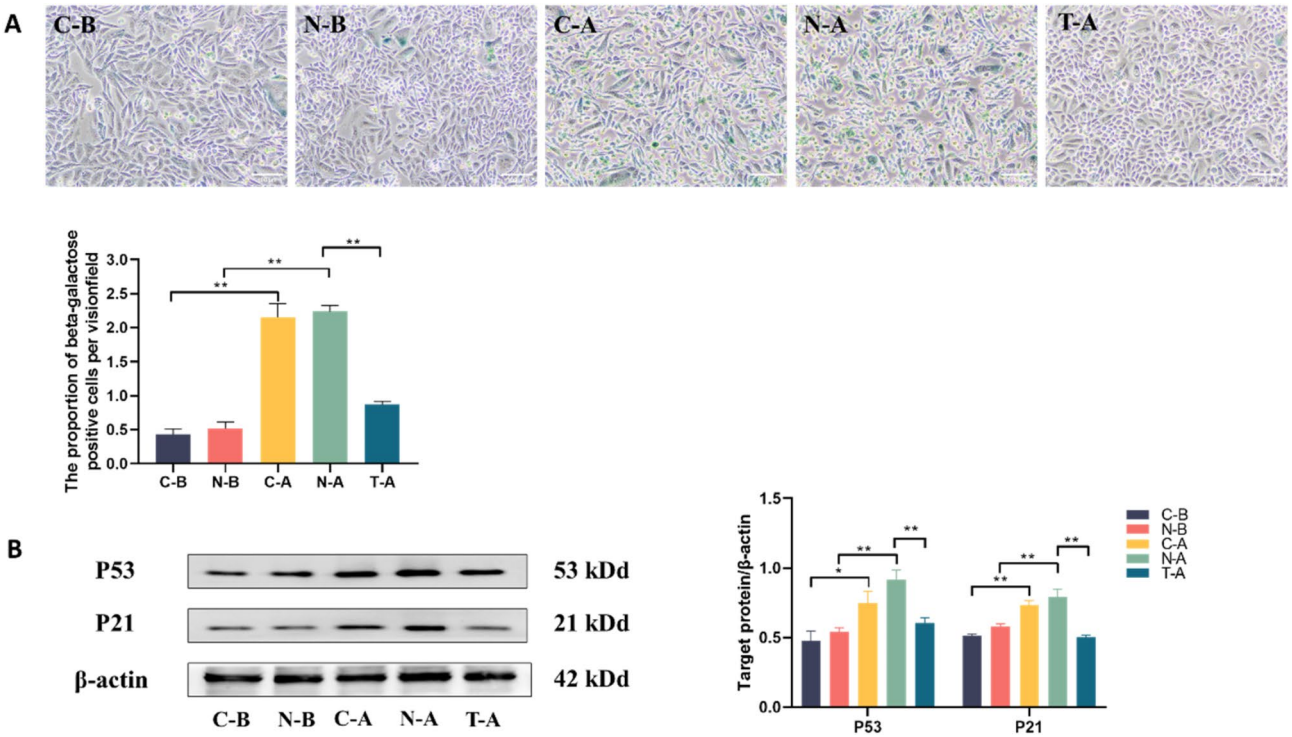

Fig. 3. Overexpression of CSTD attenuates AGEs-induced senescence in VSMCs. (**A**) Senescence-associated β-galactosidase (SA-β-Gal) staining and quantification for VSMCs (scale bar = 100 μm). (**B**) Western blot analysis of the relative expression levels of P53 and P21 in VSMCs. All data are presented as mean ± SEM ($n = 3$). * represents $p < 0.05$, ** represents $p < 0.01$.

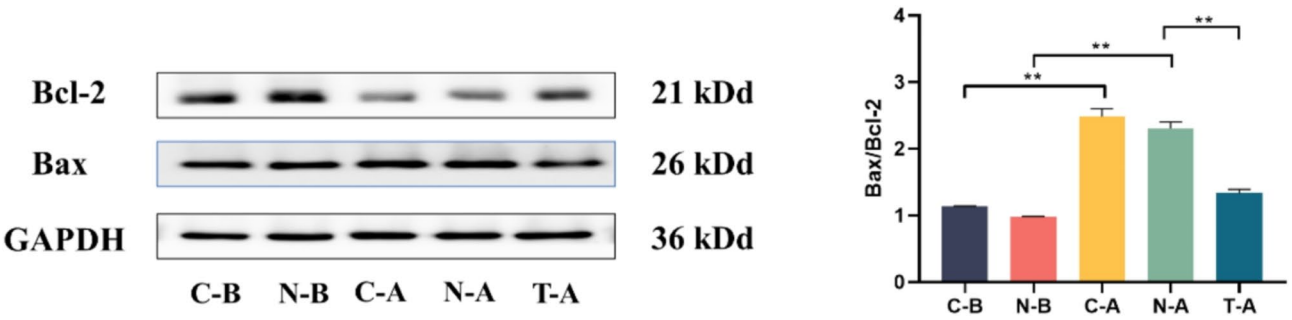

Fig. 4. Overexpression of CTSD reduces AGEs-induced apoptosis in VSMCs. Western blot analysis of the relative expression levels of Bax and BCL-2 in VSMCs. All data are presented as mean ± SEM ($n = 3$). * represents $p < 0.05$, ** represents $p < 0.01$.

246 downregulated metabolites (Fig. 7B). Compared to the N-A group, 599 DMs were identified in the T-A group, including 288 upregulated and 311 downregulated metabolites (Fig. 7B). Venn diagram analysis revealed 348 common DMs among the three groups, which may be related to the regulation of VSMC phenotypic transformation by CTSD (Fig. 7C). KEGG enrichment analysis showed that these 348 DMs were mainly enriched in glycerophospholipid metabolism (rno00564), retrograde endocannabinoid signaling (rno04723), amino sugar and nucleotide sugar metabolism (rno00520), arachidonic acid metabolism (rno00590), and glyoxylate and dicarboxylate metabolism (rno00630) (Fig. 7D).

Combined analysis of the metabolomic and transcriptomic profiles of AGEs-induced VSMCs with CTSD overexpression

Based on transcriptomic and metabolomic analyses, a combined KEGG enrichment analysis of common differentially expressed genes and differential metabolites in the N-A, N-B, and T-A groups was performed. Combined pathway analysis identified 66 pathways commonly enriched in both the transcriptome and metabolome (Fig. 8A). Among these 66 common pathways, Glucagon signaling pathway (rno04922) had the highest number of differentially expressed genes and differential metabolites (Fig. 8B). Therefore, we

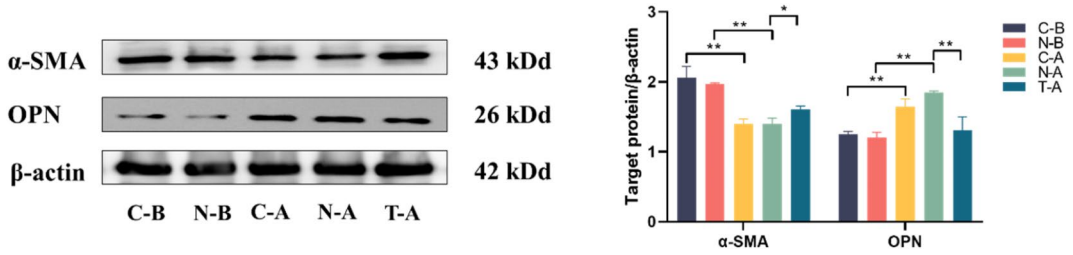

Fig. 5. Overexpression of CTSD influences VSMC phenotypic transformation through α-SMA and OPN. Western blot analysis of the relative expression levels of α-SMA and OPN in VSMCs. All data are presented as mean ± SEM ($n = 3$). * represents $p < 0.05$, ** represents $p < 0.01$. Note: α-SMA stands for Smooth muscle actin and OPN stands for Osteopontin in the figure.

hypothesize that CTSD overexpression may influence VSMC phenotypic transformation through Glucagon signaling pathway. Based on this, we examined key proteins in the glycolytic pathway of Glucagon signaling pathway using Western blot analysis. The results showed that, compared to the N-B group, the N-A group had significantly higher expression levels of GLUT1, GCK, PFKL, and PKM2. Compared to the N-A group, the T-A group had significantly lower expression levels of these proteins ($p < 0.05$) (Fig. 8C). These results indicate that CTSD overexpression may regulate VSMC phenotypic transformation by inhibiting the glycolytic process in VSMCs.

Discussion

In this study, we investigated the role of CTSD in the phenotypic transformation of AGEs-induced VSMCs. AGEs significantly inhibit the viability of VSMCs and exhibit a certain level of toxicity towards these cells (Fig. 1B and C). AGEs interact with the receptor RAGE on VSMCs, promoting their proliferation and migration, thereby playing a key role in the pathogenesis of AS[4]. Treating VSMCs with AGEs is crucial for under-standing VSMC dysfunction. AGEs treatment leads to a dose-dependent decrease in CTSD expression in VSMCs (Fig. 1D). A study on CTSD's ability to degrade AGEs-modified proteins in vitro found that AGE-modified albumin is degraded by cathepsin D; primary embryonic fibroblasts isolated from CTSD knockout animals show extensive intracellular AGE accumulation[15]. These findings suggest that CTSD may play a significant role in AGEs-induced VSMC damage.

This study found that overexpression of CTSD effectively inhibits VSMC proliferation through various methods (Fig. 2C, D, E) and also inhibits VSMC migration, although the results were not statistically significant (Fig. 2F). Ning Ye et al. found that CTSD overexpression can reduce AGEs-induced VSMC proliferation via the RAGE pathway by decreasing the levels of phosphorylated ERK[8]. Our previous research showed that CTSD overexpression protects VSMCs by restoring autophagy and inhibiting AGEs-induced proliferation, without affecting their migration ability[9]. These findings are consistent with the results of our study. However, some studies have found that during the transition of human VSMCs from a contractile to a synthetic phenotype in homogeneous cultures, the expression of proteases such as CTSD, chepsin G, and angiotensin-converting enzyme (ACE), as well as the production of angiotensin II (Ang II) and growth factors, sequentially increase, ultimately leading to VSMC proliferation[16]. After synthesis, CTSD is targeted to lysosomes to participate in protein hydrolysis, but it has also been found that CTSD can translocate from lysosomes to the cytoplasm, where it is closely related to apoptosis[17]. In-creased secretion of CTSD into the extracellular space by cancer cells enhances their invasive and metastatic potential[18]. Therefore, we hypothesize that the impact of CTSD on VSMC proliferation is closely related to its site of secretion. In this study, we constructed a VSMC model with CTSD overexpression using an overexpression vector, suggesting that CTSD may influence VSMC proliferation by regulating protein hydrolysis in lysosomes. Extracellular CTSD may have different effects on VSMC proliferation, but further experiments are needed to confirm this.

AGEs treatment increases the expression of senescence-related proteins P53 and P21, as well as the number of β-galactosidase positive cells (Fig. 3A and B), indicating that AGEs are a key factor in VSMC senescence. As individuals age, the accumulation of AGEs in the vascular wall may lead to vascular dysfunction. Senescent VSMCs exhibit increased proliferation and migration capabilities, which may promote the formation and progression of atherosclerotic plaques[19]. In our study, overexpression of CTSD significantly reduced the expression of P53 and P21 and decreased the number of β-galactosidase positive cells (Fig. 3A and B). Studies on photoaged skin have found that CTSD plays a major role in the intracellular degradation of AGEs. Reduced CTSD expression and activity impair the degradation of AGEs in photoaged fibroblasts, leading to skin aging[20]. These findings suggest that CTSD may alleviate VSMC senescence by promoting AGEs degradation, thereby regulating VSMC phenotypic transformation.

AGEs treatment significantly increases VSMC apoptosis, while CTSD overexpression effectively reduces VSMC apoptosis (Fig. 4). AGEs can induce apoptosis and stimulate calcium deposition in VSMCs through excessive oxidative stress and phenotypic trans-formation into osteoblast-like cells[5]. Vascular calcification is associated with cardiovascular disease-related mortality. Increased AGEs can activate NOX1 expression in VSMCs, inducing apoptosis and ROS production, thus playing a role in the pathogenesis of aortic dissection[21]. AGEs can cause VSMC apoptosis, which is a significant factor in the onset of cardiovascular diseases. Therefore,

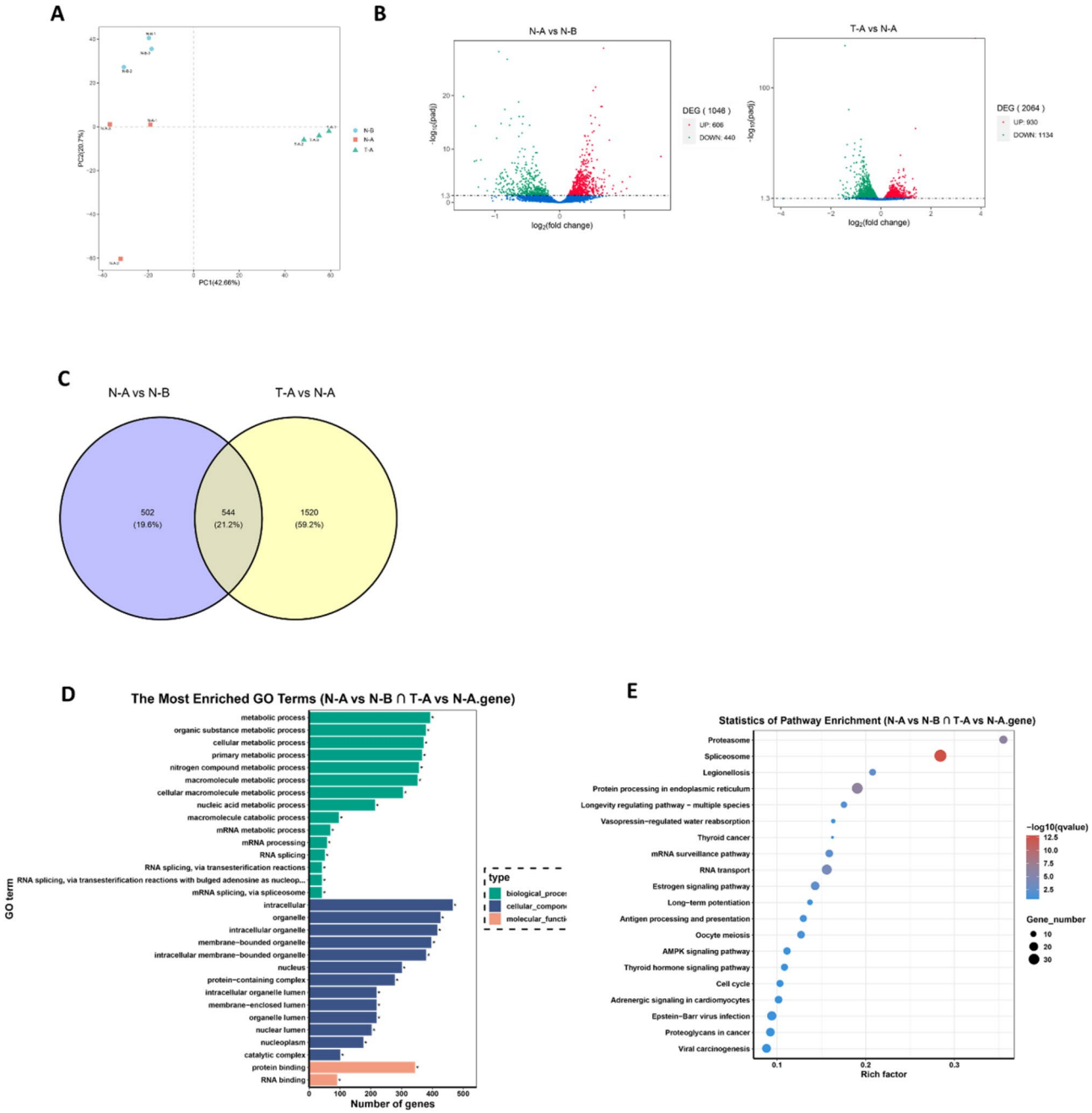

Fig. 6. Effects of CTSD overexpression on the transcriptome of AGEs-induced VSMCs. (**A**) PCA analysis of the N-A, N-B, and T-A experimental groups. (**B**) Volcano plots of differentially expressed genes in N-A vs. N-B and T-A vs. N-A. (**C**) Venn diagram of common differentially expressed genes among the N-A, N-B, and T-A groups. (**D**) GO enrichment analysis of common differentially expressed genes in the N-A, N-B, and T-A groups. (**E**) KEGG enrichment analysis of common differentially expressed genes in the N-A, N-B, and T-A groups.

inhibiting VSMC apoptosis is crucial. Transfection of the CTSD gene into mammary epithelial HC11 cells and the establishment of a stable CTSD overexpression cell line revealed that CTSD overexpression may contribute to the apoptosis of mammary epithelial cells[22]. In this study, we found that CTSD overexpression effectively reduces VSMC apoptosis, which is inconsistent with the results in mammary epithelial cells. The specific mechanisms of CTSD's action in VSMCs require further investigation.

In this study, we found that AGEs treatment significantly reduced the expression of α-SMA, while CTSD overexpression partially restored its expression (Fig. 5). α-SMA is one of the main proteins forming the cytoskeleton of VSMCs, helping to maintain the structural integrity and elasticity of blood vessels. Synthetic VSMCs enhance their proliferation and migration capabilities by downregulating α-SMA expression to participate in vascular injury repair. In vascular aging and diseases such as atherosclerosis, reduced α-SMA

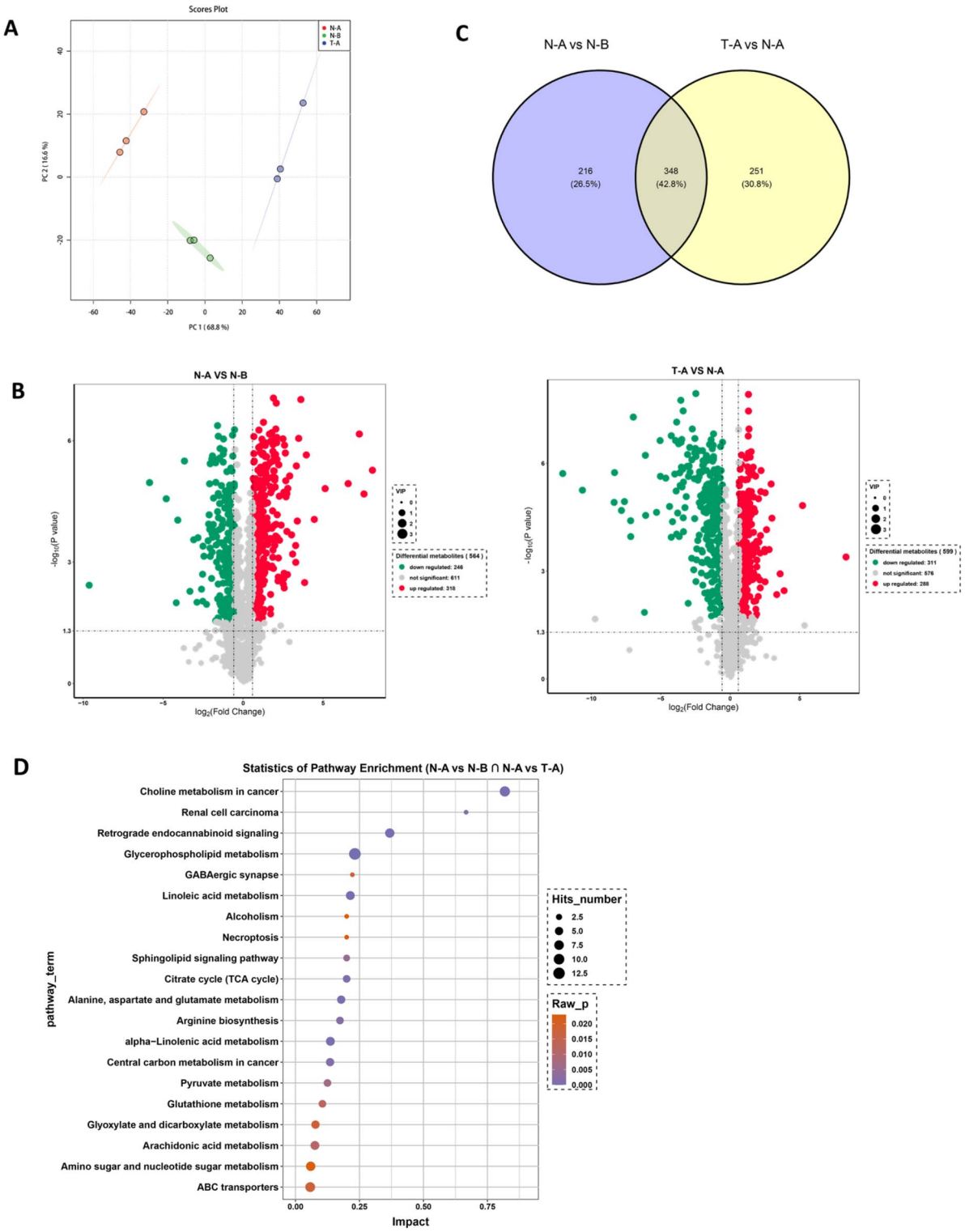

Fig. 7. Effects of CTSD overexpression on the metabolomic profile of AGEs-induced VSMCs. (**A**) PCA analysis of the N-A, N-B, and T-A experimental groups. **B** Volcano plots of differential metabolites in N-A vs. N-B and T-A vs. N-A. **C** Venn diagram of common differential metabolites among the N-A, N-B, and T-A groups. **D** Heatmap of common differential metabolites among the N-A, N-B, and T-A groups. **E** KEGG enrichment analysis of common differential metabolites among the N-A, N-B, and T-A groups.

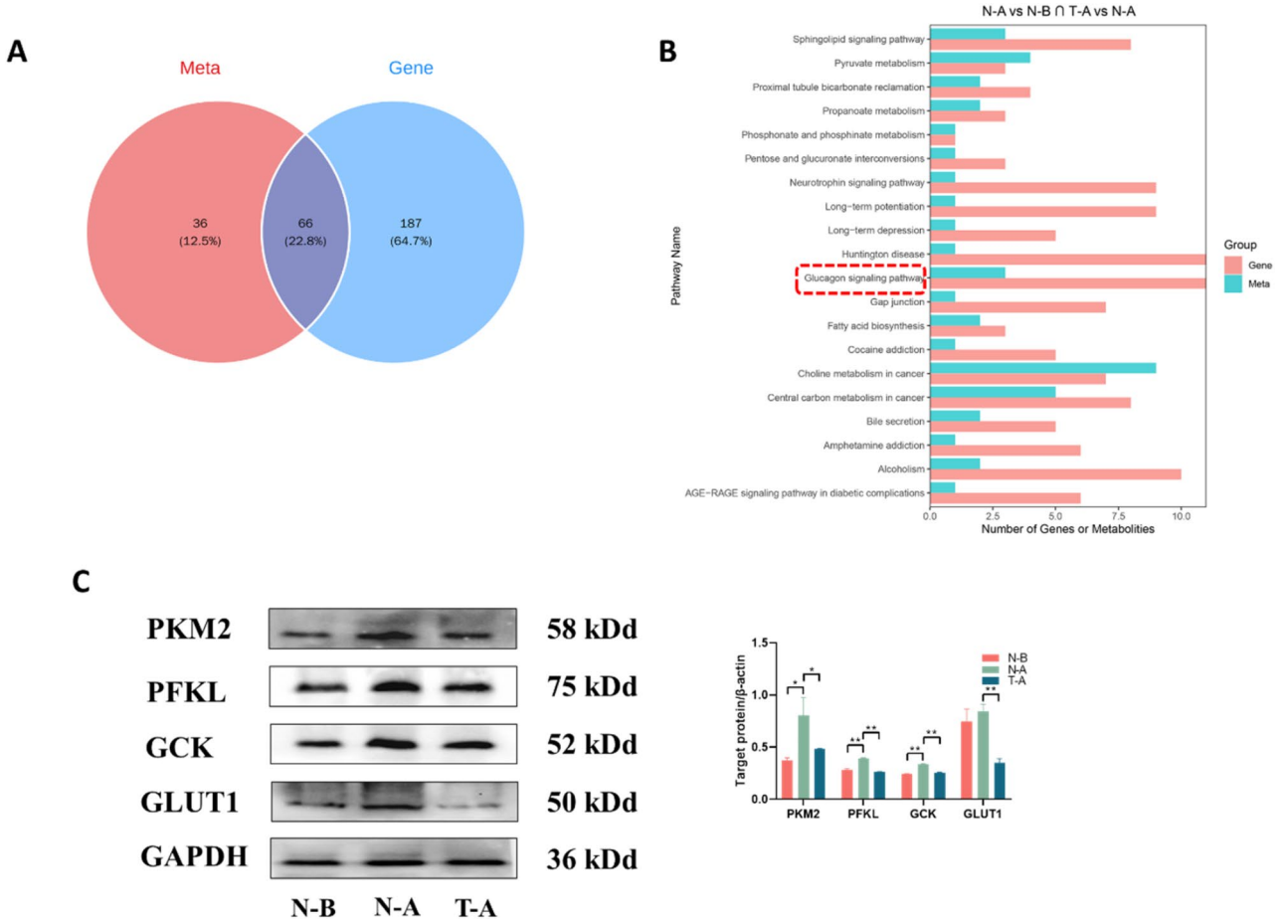

Fig. 8. Combined analysis of the metabolomic and transcriptomic profiles of AG-Es-induced VSMCs with CTSD overexpression. (**A**) Venn diagram of common KEGG enriched pathways for differentially expressed genes and differential metabolites among the N-A, N-B, and T-A groups. (**B**) Top 20 KEGG enriched pathways shared among the N-A, N-B, and T-A groups. (**C**) Relative expression levels of GLUT1, GCK, PFKL, and PKM2 in VSMCs detected by western blotting. All data are presented as mean ± SEM ($n = 3$). * represents $p < 0.05$, ** represents $p < 0.01$. Note: In the figure, GLUT1 stands for Glucose Transporter 1, GCK for Glucokinase, PFKL for Phosphofructokinase, and PKM2 for Pyruvate Kinase M2.

expression leads to VSMC dysfunction and adverse vascular structural changes[23]. CTSD is associated with α-SMA in hepatic stellate cells (HSCs) activation and liver fibrosis. During HSC activation, CTSD regulates α-SMA expression. Silencing CTSD reduces α-SMA expression, inhibiting HSC activation and proliferation. The findings from liver fibrosis studies are consistent with our conclusions, indicating that CTSD can promote α-SMA expression. Upregulating α-SMA in VSMCs may inhibit their proliferation and migration abilities[24]. OPN is a secreted protein that plays a key role in vascular injury re-pair. It is expressed at low levels under normal conditions, helping to maintain vascular health, but its expression increases under pathological conditions such as chronic inflammation and cardiovascular diseases, potentially promoting disease progression[25]. In this study, we found that AGEs treatment significantly increased OPN expression, while CTSD overexpression inhibited OPN expression (Fig. 5). Research indicates that α-SMA is an excellent marker of smooth muscle cell differentiation. Its expression decreases as VSMCs transition from a contractile to a proliferative state. OPN may regulate VSMC phenotypic changes by downregulating α-SMA and calmodulin protein expression, playing an important role in the pathogenesis of cardiovascular diseases[26]. Our findings are consistent with these studies, suggesting that CTSD may regulate VSMC phenotypic transformation by downregulating α-SMA through OPN.

To further elucidate the mechanism by which CTSD regulates VSMC phenotypic transformation, we performed transcriptomic (Fig. 6) and metabolomic (Fig. 7) analyses on CTSD-overexpressing VSMCs. A study employing a multi-omics approach that integrates single-cell transcriptomics (scRNA-seq), transcriptomics (mRNA-seq), and metabolomics (LC-MS) has deeply explored the cell types, key genes, signaling pathways, intercellular communication, and transcription factors involved in human atherosclerosis. This study revealed the complex molecular features of endothelial cells, fibroblasts, macrophages, and smooth muscle cells within atherosclerotic plaques[27]. The integration of multi-omics data enhances our understanding of disease complexity and opens new avenues for future research and clinical applications. By integrating metabolomic and transcriptomic data, we identified that the glucagon pathway might play a significant role in how CTSD regulates

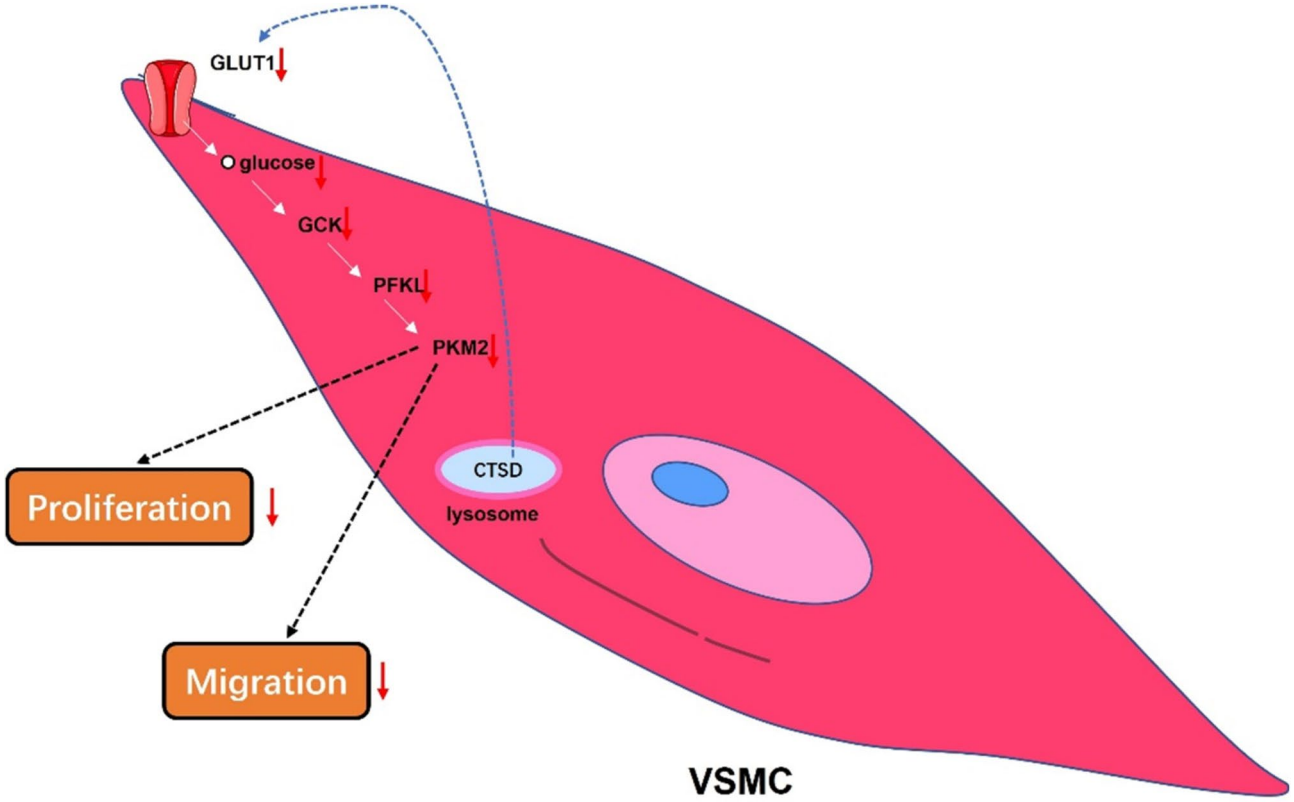

Fig. 9. Potential Mechanisms by Which CTSD Regulates Phenotypic Transformation of VSMCs through the Glycolytic Pathway.

VSMC phenotypic transformation. Further analysis of differential metabolites and genes suggests that CTSD may influence VSMC phenotypic transformation by inhibiting glycolysis (Figs. 8 and 9). Research indicates that oxidized low-density lipoprotein (ox-LDL) promotes VSMC proliferation and migration through enhancing PKM2-dependent glycolysis, thereby advancing atherosclerosis. Targeting PKM2-dependent glycolysis could provide a new therapeutic strategy for atherosclerosis[10]. Glycolysis promotes VSMC proliferation and migration, which is associated with plaque formation and instability in atherosclerosis[28]. Abnormal increases in glycolytic flux play a crucial role in atherosclerosis progression. Using inhibitors such as 3PO, PFK158, and 2-DG to regulate glycolysis can effectively slow disease progression, particularly by con-trolling excessive VSMC proliferation and migration, which significantly impacts atherosclerosis[29]. Platelet-derived growth factor (PDGF) stimulation of VSMCs increases cell migration, accompanied by enhanced glycolytic activity and upregulation of hexokinase (HK)2 expression. Inhibition of glycolysis or hexokinase significantly reduces VSMC migration[30]. The glutamine antagonist 6-diazo-5-oxo-L-norleucine (DON) significantly inhibits VSMC proliferation and migration by suppressing glycolysis and oxidative phosphorylation and reducing mTORC1 activity[31]. These studies support the conclusion that glycolysis is a key regulatory point in VSMC phenotypic transformation. This study reveals the inhibitory effect of CTSD on VSMC glycolysis, highlighting the potential of using CTSD to regulate glycolysis as a new strategy for treating atherosclerosis and providing a potential scientific basis for future research directions.

Conclusion

This study reveals the crucial role of CTSD in regulating the phenotype transformation of VSMCs. It was found that AGEs reduce CTSD expression, while overexpression of CTSD effectively inhibits VSMC proliferation and protects against AGE-induced cell migration, aging, and apoptosis. Furthermore, CTSD regulates VSMC phenotype trans-formation by partially restoring the reduced α-SMA expression caused by AGEs and inhibiting the AGE-induced upregulation of OPN. Transcriptomic and metabolomic analyses further support the mechanism by which CTSD influences VSMC phenotype trans-formation through the inhibition of glycolysis. Therefore, CTSD offers a new perspective for treating cardiovascular diseases associated with diabetes and may serve as a new tar-get for therapeutic strategies. However, its specific molecular mechanisms in VSMC phenotype transformation and clinical application prospects require further research and validation.

Data availability

The datasets used in the current study are available from the corresponding author on reasonable request. The datasets generated and/or analyzed during the current study are available in the [GEO] repository [Accession Number: GSE278266] https://www.ncbi.nlm.nih.gov/geo/query/acc.cgi? acc=GSE278266.

Received: 9 September 2024; Accepted: 25 March 2025
Published online: 03 April 2025

References

1. Wang, D. et al. Nox4 as a novel therapeutic target for diabetic vascular complications. *Redox Biol.* **64**, 102781. https://doi.org/10.1016/j.redox.2023.102781 (2023).
2. Maruhashi, T. & Higashi, Y. Pathophysiological association between diabetes mellitus and endothelial dysfunction. *Antioxidants* **10** (8), 1306. https://doi.org/10.3390/antiox10081306 (2021).
3. Khalid, M., Petroianu, G. & Adem, A. Advanced glycation end products and diabetes mellitus: Mechanisms and perspectives. *Biomolecules* **12** (4), 542. https://doi.org/10.3390/biom12040542 (2022).
4. Mao, L., Yin, R., Yang, L. & Zhao, D. Role of advanced glycation end products on vascular smooth muscle cells under diabetic atherosclerosis. *Front. Endocrinol.* **13**, 983723. https://doi.org/10.3389/fendo.2022.983723 (2022).
5. Koike, S. et al. Advanced glycation end-products induce apoptosis of vascular smooth muscle cells: A mechanism for vascular calcification. *Int. J. Mol. Sci.* **17** (9), 1567. https://doi.org/10.3390/ijms17091567 (2016).
6. Tang, H. Y. et al. Vascular smooth muscle cells phenotypic switching in cardiovascular diseases. *Cells* **11** (24), 4060. https://doi.org/10.3390/cells11244060 (2022).
7. Benes, P., Vetvicka, V. & Fusek, M. Cathepsin D—many functions of one aspartic protease. *Crit. Rev. Oncol. Hematol.* **68** (1), 12–28. https://doi.org/10.1016/j.critrevonc.2008.02.008 (2008).
8. Ye, N. et al. Cathepsin D attenuates the proliferation of vascular smooth muscle cells induced by the AGE/RAGE pathway by suppressing the ERK signal. *Curr. Pharm. Design.* **29** (30), 2387–2395. https://doi.org/10.2174/0113816128261894231012144719 (2023).
9. Ma, M. et al. Advanced glycation end products promote proliferation and suppress autophagy via reduction of cathepsin D in rat vascular smooth muscle cells. **403**(73–83. (2015). https://doi.org/10.1007/s11010-015-2338-x
10. Zhao, X. et al. PKM2-dependent Glycolysis promotes the proliferation and migration of vascular smooth muscle cells during atherosclerosis. *Acta Biochim. Biophys. Sin.* **52** (1), 9–17. https://doi.org/10.1093/abbs/gmz135 (2020).
11. Zhang, X. et al. KLF4-PFKFB3-driven Glycolysis is essential for phenotypic switching of vascular smooth muscle cells. *Commun. Biology*. **5** (1), 1332. https://doi.org/10.1038/s42003-022-04302-y (2022).
12. Cavill, R., Jennen, D., Kleinjans, J. & Briedé, J. J. Transcriptomic and metabolomic data integration. *Brief. Bioinform.* **17** (5), 891–901. https://doi.org/10.1093/bib/bbv090 (2016).
13. de Silva, O. Modulation of CD36 protein expression by ages and insulin in aortic VSMCs from diabetic and non-diabetic rats. *Nutr. Metabolism Cardiovasc. Dis.* **18** (1), 23–30 (2008).
14. Chen, X. et al. Overexpression of UHRF1 promoted the proliferation of vascular smooth cells via the regulation of Geminin protein levels. *Biosci. Rep.* **39** (2), BSR20181341 (2019).
15. Grimm, S. et al. Cathepsin D is one of the major enzymes involved in intracellular degradation of AGE-modified proteins. *Free Radic. Res.* **44** (9), 1013–1026. https://doi.org/10.3109/10715762.2010.495127 (2010).
16. Hu, W. Y. et al. Human-derived vascular smooth muscle cells produce angiotensin II by changing to the synthetic phenotype. *J. Cell. Physiol.* **196** (2), 284–292. https://doi.org/10.1002/jcp.10299 (2003).
17. Zaidi, N., Maurer, A., Nieke, S. & Kalbacher, H. Cathepsin D: A cellular roadmap. *Biochem. Biophys. Res. Commun.* **376** (1), 5–9. https://doi.org/10.1016/j.bbrc.2008.08.099 (2008).
18. Koblinski, J. E., Ahram, M. & Sloane, B. F. Unraveling the role of proteases in cancer. *J. Clin. Chim. Acta*. **291** (2), 113–135. https://doi.org/10.1016/S0009-8981(99)00224-7 (2000).
19. Monk, B. A. & George, S. J. The effect of ageing on vascular smooth muscle cell behaviour-a mini-review. *Gerontology* **61** (5), 416–426. https://doi.org/10.1159/000368576 (2015).
20. Xu, X. et al. Cathepsin D contributes to the accumulation of advanced glycation end products during Photoaging. *J. Dermatol. Sci.* **90** (3), 263–275. https://doi.org/10.1016/j.jdermsci.2018.02.009 (2018).
21. Wei, Z. et al. The role of AGEs-RAGE in the regulation of VSMC apoptosis in arterial dissection. *Int. J. Clin. Exp. Med.* **12** (7), 8654–8661 (2019).
22. Seol, M., Bong, J. & Baik, M. Involvement of cathepsin D in apoptosis of mammary epithelial cells. *Asian-australasian J. Anim. Sci.* **19** (8), 1100–1105. https://doi.org/10.5713/ajas.2006.1100 (2006).
23. Cao, G. et al. How vascular smooth muscle cell phenotype switching contributes to vascular disease. *Cell. Communication Signal.* **20** (1), 180. https://doi.org/10.1186/s12964-022-00993-2 (2022).
24. Moles, A., Tarrats, N., Fernández-Checa, J. C. & Marí, M. Cathepsins B and D drive hepatic stellate cell proliferation and promote their fibrogenic potential. *Hepatology* **49** (4), 1297–1307. https://doi.org/10.1002/hep.22753 (2009).
25. Lok, Z. S. Y. & Lyle, A. N. Osteopontin in vascular disease: Friend or foe? *Arteriosclerosis, thrombosis, vascular biology* 39(4), 613–622. (2019). https://doi.org/10.1161/ATVBAHA.118.311577
26. Gao, H., Steffen, M. C. & Ramos, K. S. Osteopontin regulates α-smooth muscle actin and Calponin in vascular smooth muscle cells. *Cell. Biol. Int.* **36** (2), 155–161. https://doi.org/10.1042/CBI20100240 (2012).
27. Liu, X., Li, L., Yin, Y., Zhang, L. & Wang, W. Single-cell transcriptomic, transcriptomic, and metabolomic characterization of human atherosclerosis. *Annals Translational Med.* **10** (22), 1215. https://doi.org/10.21037/atm-22-4852 (2022).
28. Xu, R., Yuan, W. & Wang, Z. Advances in Glycolysis metabolism of atherosclerosis. *J. Cardiovasc. Transl. Res.* **16** (2), 476–490. https://doi.org/10.1007/s12265-022-10311-3 (2023).
29. Li, L., Wang, M., Ma, Q., Ye, J. & Sun, G. Role of Glycolysis in the development of atherosclerosis. *Am. J. Physiology-Cell Physiol.* **323** (2), C617–C629. https://doi.org/10.1152/ajpcell.00218.2022 (2022).
30. Heiss, E. H., Schachner, D., Donati, M., Grojer, C. S. & Dirsch, V. M. Increased aerobic Glycolysis is important for the motility of activated VSMC and inhibited by indirubin-3′-monoxime. *Vascul. Pharmacol.* **83**, 47–56. https://doi.org/10.1016/j.vph.2016.05.002 (2016).
31. Park, H. Y. et al. Inhibitory effect of a glutamine antagonist on proliferation and migration of VSMCs via simultaneous Attenuation of Glycolysis and oxidative phosphorylation. *Int. J. Mol. Sci.* **22** (11), 5602. https://doi.org/10.3390/ijms22115602 (2021).

Author contributions

Conceptualization: X.H. and S.T.; Methodology: S.T. and M.M.; Validation: X.H., S.T., and L.B.; Writing - original draft: X.H., S.T., and X.Z.; Writing - review & editing: R.G., M.M., and L.Z.; Data curation: X.H., L.B., and P.Z.; Software: S.T., L.B., and X.Z.; Resources: S.T., X.H., and P.Z.; Super-vision: R.G., M.M., and L.Z.; Project administration: M.M. and R.G.; Funding acquisition: R.G. and M.M. All authors have read and agreed to the published version of the manuscript.

Funding

This research was funded by the Supported by Fundamental Research Program of Shanxi Province

(201901D111471), the Lvliang introduces high-level scientific and technological talents to focus on research and development project (2019115), and the Fenyang College of Shanxi Medical University 2024 Doctoral Research Initiation Grant Program (2024BS09).

Declarations

Competing interests

The authors declare no competing interests.

Additional information

Supplementary Information The online version contains supplementary material available at https://doi.org/10.1038/s41598-025-96038-y.

Correspondence and requests for materials should be addressed to R.G. or M.M.

Reprints and permissions information is available at www.nature.com/reprints.

Publisher's note Springer Nature remains neutral with regard to jurisdictional claims in published maps and institutional affiliations.